Quaternary Science Reviews 29 (2010) 3861–3874

Contents lists available at ScienceDirect

Quaternary Science Reviews

journal homepage: www.elsevier.com/locate/quascirev

Using proglacial-threshold lakes to constrain fluctuations of the Jakobshavn Isbræ ice margin, western Greenland, during the Holocene

J.P. Briner*, H.A.M. Stewart, N.E. Young, W. Philipps, S. Losee

Department of Geological Sciences, University at Buffalo, 411 Cooke Hall, Buffalo, NY 14260, United States

ARTICLE INFO

Article history:
Received 27 June 2010
Received in revised form
2 September 2010
Accepted 8 September 2010

ABSTRACT

The future response of the Greenland Ice Sheet (GIS) and its potential contribution to sea level rise are uncertain. Rapid changes of Greenland's outlet glaciers over the past decade have made it difficult to extrapolate ice sheet change into the future. This significant short-term variability highlights the need for longer-term, geologic (e.g., Holocene) records of ice margin fluctuations. However, a major challenge with reconstructing the GIS during the Holocene stems from it having been smaller than it is at present, thus traditional glacial geologic approaches are not suitable. We use radiocarbon-dated sediment sequences from seven proglacial-threshold lakes spanning ~50 km of the western GIS margin near Jakobshavn Isbræ to constrain the timing of early Holocene deglaciation, the duration that this sector of the western GIS was smaller than its present configuration, and the timing of its advance during Neoglaciation. Our reconstructions suggest deglaciation ~7300 cal yr BP, minimum ice extent ~6000–5000 cal yr BP and smaller-than-present ice configuration until at least ~2300 cal yr BP for the ice margin south of Jakobshavn Isbræ, and until ~400 cal yr BP for the ice margin north of Jakobshavn Isbræ. One relatively large proglacial lake that became briefly ice-free during the middle Holocene lies in a catchment that likely extends 10s of km inland beneath the GIS, suggesting significant middle Holocene retreat of this portion of the GIS. The overall pattern of ice sheet change is inconsistent with existing ice sheet model reconstructions for this region, but is consistent with numerous paleoclimate proxy and relative sea level data. These continuous lacustrine records corroborate, but provide closer age control than, existing non-continuous records of radiocarbon-dated reworked bivalves from historical moraines in the region. Reconstructing ice margin change from proglacial-threshold lakes is one of few approaches with the potential to constrain smaller-than-present ice sheet extent.

1. Introduction

The cryosphere plays a critical role in the earth system, both in terms of cryosphere-albedo feedbacks that amplify warming in the Arctic (ACIA, 2005; Chapin et al., 2005; Miller et al., 2010) and as a major contributor to global sea level rise via melting glaciers and ice sheets that sensitively respond to climate change (Alley et al., 2005; IPCC, 2007; Meier et al., 2007). Paleo-records of climate and ice sheet change place empirical constraints on climate sensitivity and the magnitude of climate feedbacks, the magnitude of ice sheet and sea level responses to temperature changes, and spatial variability of earth systems in response to radiative forcing (e.g., Kaufman et al., 2004, 2009; CAPE, 2006; Otto-Bliesner et al., 2006; Overpeck et al., 2006). Reconstructions of cryospheric change during past periods warmer than today (e.g., the early and middle Holocene, when climatic boundary conditions were generally similar to present), have clear relevance to forecasting the impacts of ongoing and future warming. In particular, the Greenland Ice Sheet (GIS; Fig. 1) has been directly implicated in altering global oceanic circulation, driving abrupt climate change and causing rapid sea level rise (Alley et al., 2005, 2010; IPCC, 2007; Rignot et al., 2008; Long, 2009).

Recent studies reveal a slightly thickening interior and dramatic coastal thinning of the GIS, with overall increasingly negative mass balance over the last decade (Krabill et al., 2004; Zwally et al., 2005; Box et al., 2006; Thomas et al., 2006). The GIS alone is estimated to be currently contributing a few tenths of a mm yr^{-1}, and may contribute tens of cm by century's end (Parizek and Alley, 2004; Meier et al., 2007; Pfeffer et al., 2008; Long, 2009). However, our incomplete understanding of dynamic processes that are important components of the ice sheet's mass balance lead to large uncertainties in forecasts of the ice sheet's contribution to future sea level change (Alley et al., 2005; IPCC, 2007; Nick et al., 2009). The rapid shifts in velocity of GIS outlet glaciers over the last decade have

* Corresponding author.
E-mail address: jbriner@buffalo.edu (J.P. Briner).

0277-3791/$ – see front matter © 2010 Elsevier Ltd. All rights reserved.
doi:10.1016/j.quascirev.2010.09.005

revealed how dynamic the ice sheet's behavior can be (Joughin et al., 2004; Rignot and Kanagaratnam, 2006; Howat et al., 2007; Pritchard et al., 2009).

Jakobshavn Isbræ is the GIS' largest outlet glacier, draining an estimated 6.5% of the present ice sheet area (Rignot and Kanagaratnam, 2006), and producing more than 10% of the total GIS iceberg output (Weidick and Bennike, 2007). Since 1850 AD, observations of calving front positions have been established for Jakobshavn Isbræ, and in the last 150 years, Jakobshavn Isbræ's calving terminus has retreated approximately 35 km (Joughin et al., 2004; Howat et al., 2007; Weidick and Bennike, 2007; Csatho et al., 2007). Particularly dramatic changes in ice margin retreat and acceleration in the last decade have revealed the dynamic nature of Jakobshavn Isbræ (Rignot and Kanagaratnam, 2006; Howat et al., 2007; Holland et al., 2008), and warrant investigation of Jakobshavn Isbræ's behavior and links to climate change on longer timescales. The details of Jakobshavn Isbræ's behavior are unknown prior the satellite era, and even generalized information about ice margin location is very poorly known prior to 1850 AD.

Here, we develop radiocarbon-dated lake sediment records from seven proglacial-threshold lakes near Jakobshavn Isbræ to constrain its terminus location during the Holocene. We build on the initial findings reported by Young et al. (in press), which combines the chronology from one lake with 18 cosmogenic ^{10}Be exposure ages of early Holocene deglaciation. We find that following early Holocene deglaciation, the Jakobshavn ice margin was farther inland than today until the Little Ice Age (LIA; 1250–1900 AD), when the maximum Neoglacial extent was achieved. We studied one large proglacial lake that lies within a large catchment area, and find that minimum ice extent was achieved ~6–5 ka, after which time this sector of the western GIS began to expand.

2. Setting and glacial history

Jakobshavn Isbræ is located on the west-central coast of Greenland (Fig. 1) and drains into Disko Bugt, which lies between the west-central Greenland coastline and the continental shelf of Baffin Bay. Between the ice margin around Jakobshavn Isbræ and Disko Bugt is an ice-free strip of land 40–50 km wide containing ice-sculpted bedrock dotted with hundreds of lakes. The ice-free area between the Jakobshavn Isbræ and Disko Bugt is dissected by Jakobshavn Isfjord, which has tributary fjords entering from the north and south (Fig. 1).

Field-based reconstructions of deglaciation following the Last Glacial Maximum (LGM) reveal that the western GIS was retreating throughout most of the early Holocene (e.g., Funder and Hansen, 1996; Bennike and Bjork, 2002; Funder et al., 2004; Weidick et al., 2004). The post-LGM history of Jakobshavn Isbræ is based on radiocarbon ages from marine cores, raised marine sediments

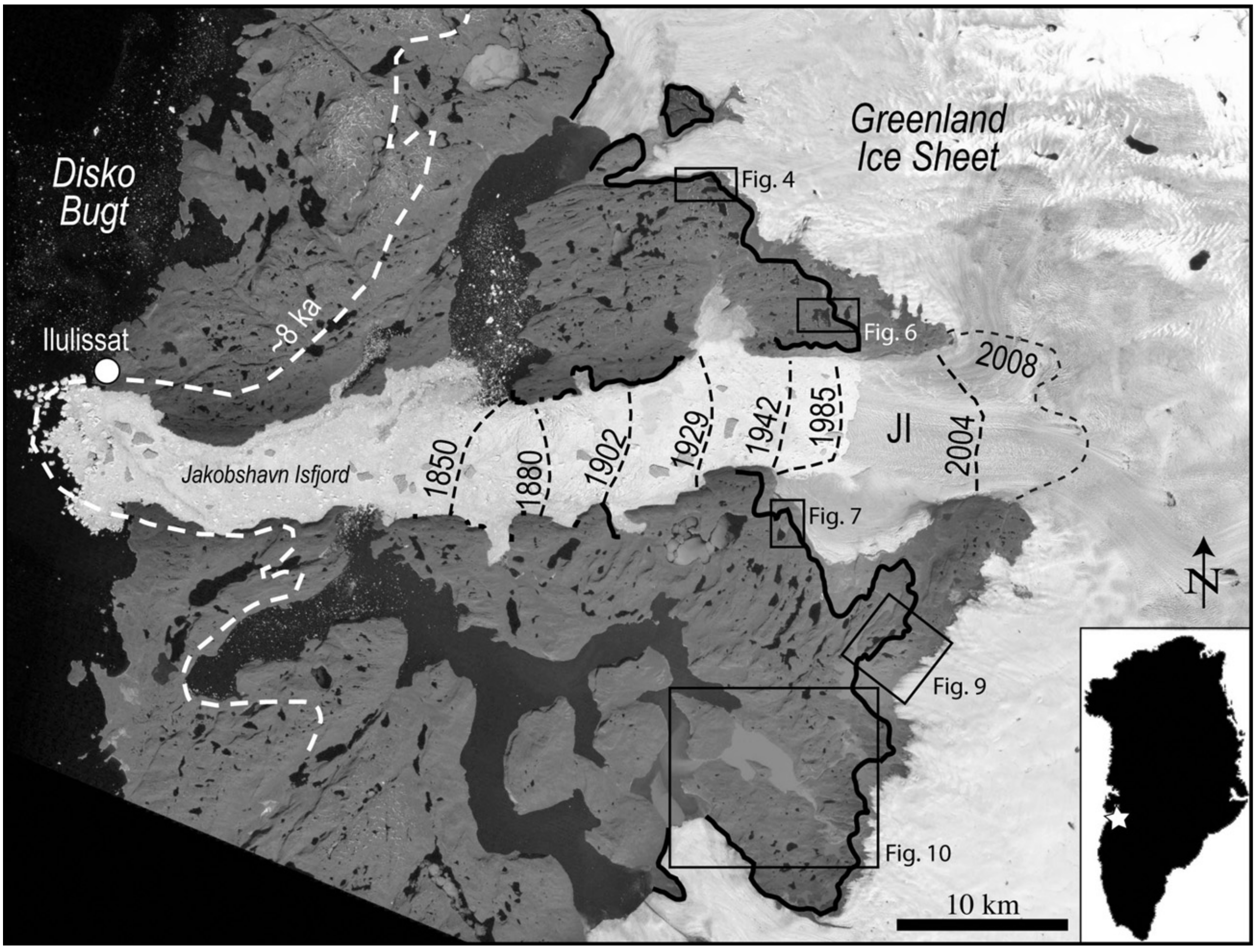

Fig. 1. Jakobshavn Isfjord region showing inner Fjord-Stade moraine (white dashed line; from Weidick and Bennike, 2007), the maximum extent of ice during Neoglaciation (historical moraine = black line) and various calving terminus locations of Jakobshavn Isbræ (JI; dashed black lines; Csatho et al., 2007). One estimate for the minimum extent of ice during the middle Holocene from Weidick et al. (1990) is shown as the dotted black line. Basemap is Landsat image from 2000 AD; inset shows location of the map area on western Greenland.

and basal lake sediments (Weidick, 1974; Bennike et al., 1994; Lloyd et al., 2005; Long et al., 2006; Weidick and Bennike, 2007). Deglaciation of the continental shelf occurred around 11–10 ka, and ice retreated from Disko Bugt and onto land by 9.9–9.6 ka (Bennike and Bjork, 2002; Lloyd et al., 2005). Evidence for advances or standstills of the ice sheet margin is recorded by the "Fjord-Stade" moraines, which are traceable for over 100 km north and south of Jakobshavn Isfjord (Weidick, 1968; Long and Roberts, 2002; Young et al., in press). The Fjord-Stade moraines have been constrained with radiocarbon dating from raised marine deposits and basal lake sediments to be between ~9.5 and ~7.7 ka (Long and Roberts, 2002; Long et al., 2006; Weidick and Bennike, 2007). Young et al. (in press) dated the younger of the two moraines to ~8.2 ka, and subsequent retreat of the ice margin to a location behind its Neoglacial maximum position by 7.4 ± 0.1 ka.

During the middle Holocene, Jakobshavn Isbræ's margin is thought to have been behind its present position (Weidick et al., 1990; Weidick, 1992). But, reconstructing the exact GIS extent between early Holocene deglaciation and the late Holocene maximum extent is challenging because the glacial geologic record is obscured beneath the present-day GIS. Despite the challenge, some field data provide useful constraints. For example, subfossil marine fauna (e.g., bivalves) reworked into late Holocene moraines requires open water conditions farther inland, indicating recent ice advances through previously ice-free fjords (Weidick et al., 1990; Weidick, 1992). Radiocarbon ages of this reworked material constrain portions of time with smaller-than-present ice extents, and constrain Jakobshavn Isbræ to be somewhere inland of its present position between ~6100 and ~2300 cal yr BP (Weidick and Bennike, 2007).

The pattern of GIS expansion during the late Holocene is not well known, but research to date suggests a variable response across western Greenland. For example, in many areas the maximum Neoglacial extent was achieved during the LIA, recognized on the landscape as the 'historical moraine' (Weidick, 1968; Kelly, 1980; Kaplan et al., 2002). However, other sectors of the western GIS seem to have attained a maximum extent prior to the LIA, perhaps ~2000 yr ago (Kelly, 1980; Bennike and Sparrenbom, 2007; Forman et al., 2007; Weidick and Bennike, 2007). Relative sea level curves in the Jakobshavn region show submergence of the landscape beginning ~3 ka, which is interpreted as GIS expansion during Neoglaciation (Weidick, 1994; Long and Roberts, 2003; Long et al., 2006). Thus, although the broad timing and pattern of western GIS changes are known, more precise information about the time period over which ice was smaller than at present and the duration that this sector of the GIS has been near its present limit is unknown.

3. Approach and methods

We constrain the timing of early Holocene retreat and subsequent ice margin position using sediment cores from "proglacial-threshold" lakes. These are lakes that have had their drainage basins partially occupied by advancing ice such that they transition from being non-glacial lakes to proglacial (glacier fed) lakes; the lakes themselves are not overridden by ice (Fig. 2). Thus, proglacial-threshold lakes contain non-glacial, organic-rich sediments during intervals of relatively restricted ice extent, and proglacial, minerogenic-rich sediments when ice is relatively extensive (Kaplan et al., 2002; Daigle and Kaufman, 2009). One caveat with this approach is that information about ice margin change is limited to the lake's drainage basin. Thus, when the ice sheet margin lies outside of a lake's catchment, the lake sediments cannot be used to determine the location of the ice sheet margin. Nonetheless, this "binary" signal still places constraints on periods of ice margin change when the ice margin resides within a threshold lake's drainage basin.

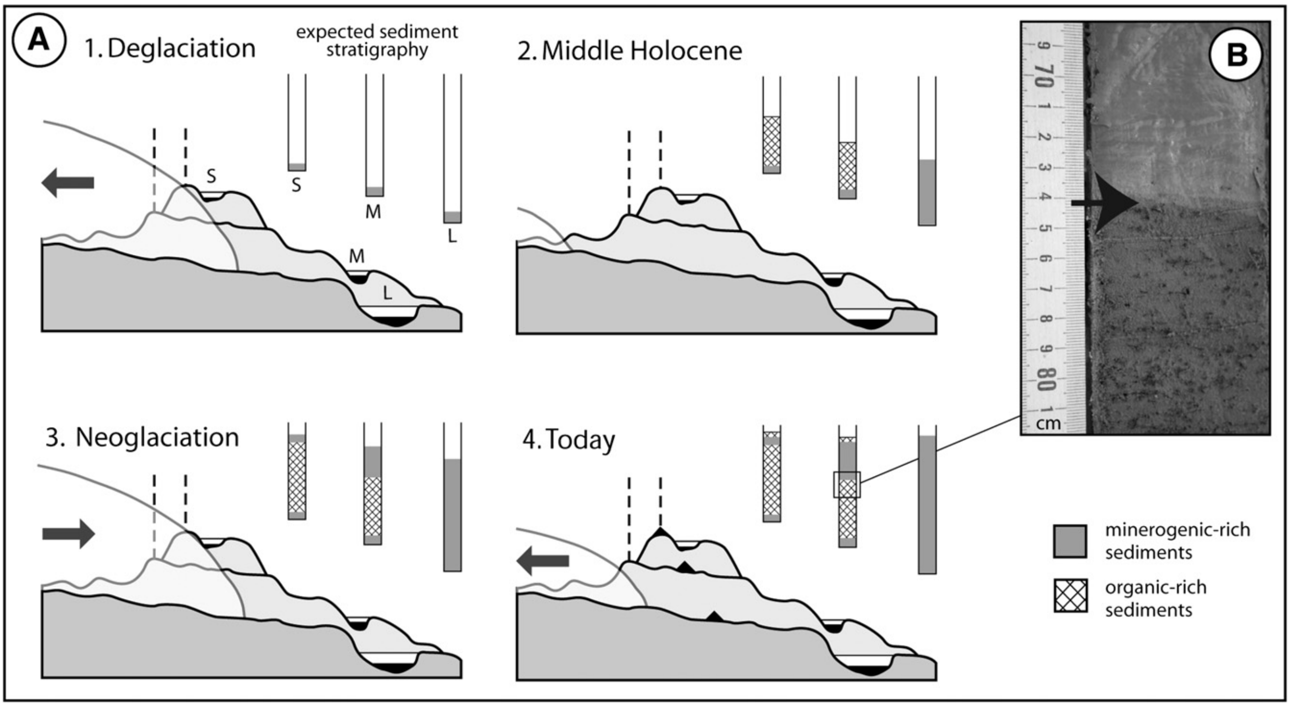

Fig. 2. A. Schematic topographic cross-sections illustrating how proglacial-threshold lakes are used to reconstruct ice margin history. Topographic thresholds (vertical dashed lines) of small lake catchments (S) are only crossed by ice when it is very near its maximum position; topographic thresholds of medium-sized lake catchments (M) are crossed later during retreat and earlier during advance; large (L) lake catchments are glaciated the longest during retreat and advance. Adjacent to each cross-section are hypothetical sediment sequences from each lake size category; black triangles on the final panel represent the historic moraine. B. Photograph of 08GOO-4 as an example of the sharpness of organic-rich to minerogenic-rich sedimentary contacts that is typical of proglacial-threshold lakes.

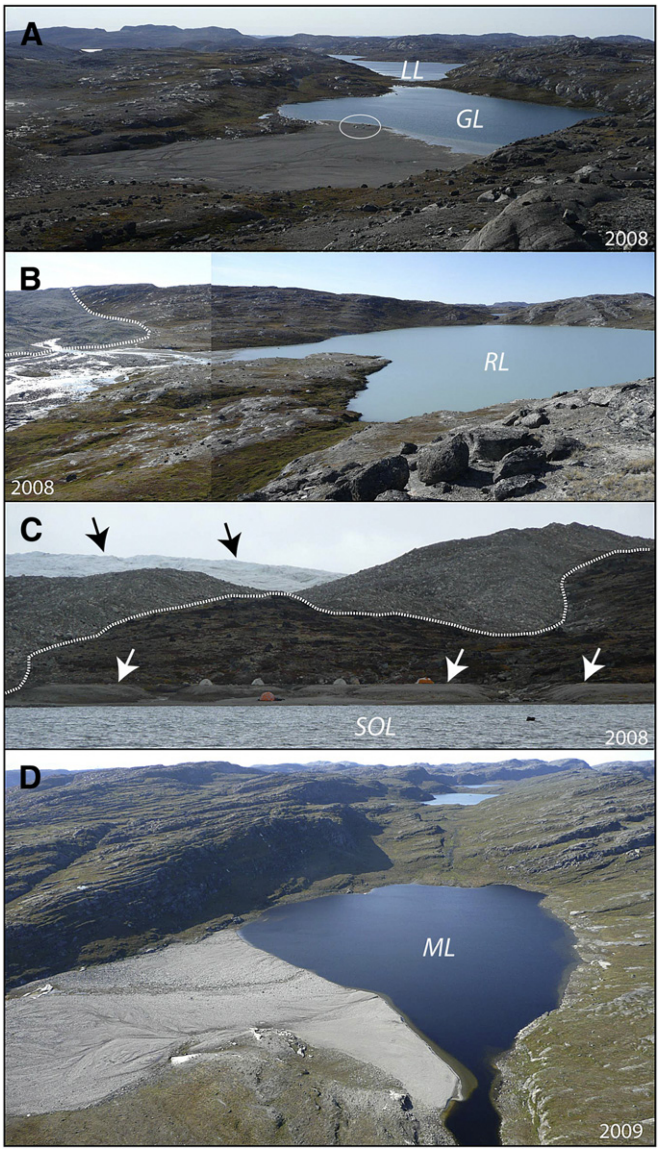

Fig. 3. Photographs of proglacial-threshold lakes in the field area. A. Goose Lake (GL) and Loon Lake (LL); a delta associated with the historic moraine can be seen adjacent to GL; circle encloses four tents for scale. B. Raven Lake (RL) lies adjacent to the historic moraine (white dotted line); Raven Lake's outflow and inflow occur in the same area, which can be seen on the left side of the photograph. C. View of eastern shoreline of South Oval Lake (SOL); raised delta surface highlighted with arrows; tents for scale. The ice sheet can be seen in the distance (black arrows), and the extent of the historic drift is delineated by dotted white line. D. Aerial view of Merganser Lake (ML) and the substantial proglacial delta that prograded into the lake during the emplacement of the historical moraine (delta front is 0.5 km wide).

Furthermore, coring multiple lakes with different catchment sizes potentially provides additional information on ice margin geometry (Fig. 2). Finally, by investigating multiple lakes along an ice margin, the spatial component of ice margin change can be assessed.

We cored seven lakes that span ~50 km of the western GIS margin near Jakobshavn Isbræ (Figs. 1 and 3), which were chosen by consulting aerial photographs. Two lakes are proglacial, whereas five are presently non-glacial. Most lakes that we cored lie in small catchments (<10 km^2) that are only beached by ice when it is near its Neoglacial maximum extent. However, we cored one proglacial lake with a large catchment area (the ice-free potion of the catchment is >70 km^2), to determine if ice ever retreated far enough inland during the Holocene to leave this catchment ice-free. The transition from proglacial to non-glacial conditions during 20th century ice margin retreat is constrained by aerial imagery for two lakes. Glacial geologic mapping from aerial photographs indicated that all lakes that are presently non-glacial were proglacial lakes during the emplacement of the historical moraine.

We cored five of the study lakes in summer 2008, and two in summer 2009. Lake bathymetry was collected using a weighted tape measure (3 lakes) or recorded using a Garmin GPSMAP 400 series GPS receiver connected to a dual beam depth transducer (4 lakes). Bathymetric maps were created by importing GPS-derived waypoints into the ArcGIS package where contours were generated automatically, note that contours away from bathymetric measurements are poorly constrained. Coring was executed using a Universal Coring system and a Nesje-style percussion-piston coring system (Nesje, 1992); we collected the sediment–water interface from all lakes. In surface cores, the water above the surface sediments was iteratively drained using a small awl hole at the interface as the sediment cores were kept vertical for several days. Sediment cores were subsequently packed with foam and capped for transport and cold storage at the University at Buffalo. Upon splitting, each core was immediately photographed with a digital camera and tripod and logged to scale. Magnetic susceptibility (MS), a measure of the relative amount of minerogenic material in the sediment, was performed on all split cores at 0.5 cm contiguous intervals using a Bartington MS2E High Resolution Surface Scanning Sensor scanner connected to a Bartington MS2 Magnetic Susceptibility Meter. Percent loss-on-ignition (LOI) at 550 °C, a measure of sediment organic matter content, was measured on an aliquot of freeze-dried sub-samples collected every 0.5 cm from selected cores.

We report 17 radiocarbon ages from lake sediments, and one radiocarbon age of a marine bivalve from raised marine deposits. Macrofossils were picked and cleaned with de-ionized water and sent to the INSTAAR (University of Colorado) Laboratory for AMS Radiocarbon Preparation and Research for AMS radiocarbon dating. The humic acid fraction was extracted from bulk sediments for AMS analysis in locations where macrofossils are absent ($n = 2$). We calibrated all ages using CALIB html version 6.0 with INTCAL09 (Stuiver et al., 2005). The bivalve was calibrated with MARINE09 and a ΔR value of 140 yr (McNeely et al., 2006). We report the mean age with two-standard deviation uncertainty, calculated by taking the midpoint of the two-standard deviation range, as well as the two-standard deviation age range solutions (Table 1).

4. Proglacial-threshold lakes

4.1. South Oval Lake

South Oval Lake [informal name, ~290 m above sea level (asl)] is the northernmost lake that we studied (Fig. 4). The historical moraine is draped across a bedrock drainage divide at the lake's eastern shoreline; the present ice margin lies ~1 km farther to the east. South Oval Lake lies in a 0.85 km^2 catchment, and has a single outflow along its southernmost shoreline. South Oval Lake level was higher during emplacement of the historical moraine, revealed by a prominent inflow delta and shorelines rimming the basin ~3 m-higher than present lake level. The lake has complex bathymetry controlled by bedrock structure striking west–northwest/east–southeast. A relatively shallow, broad basin at 6–8 m depth comprises the eastern portion of the lake, which is separated by shallow bedrock structures from basins up to 16 m-deep on the western side of the lake.

We collected two sediment cores from South Oval Lake. Core 08SOV-1 (69°18′32″ N, 50°11′11″ W) was collected from 6.74 m

Table 1
Radiocarbon ages from lake sediment cores.

Core	Depth (cm)	Lab Number	Material Dated	Fraction Modern	δ13C (‰PDB)	Radiocarbon Age (14C yr BP)	Calibrated Age (cal yr BP ± 2σ)	Calibrated Age Ranges (cal yr BP ± 2σ)
Loon Lake								
08LOO-1	20	CURL-10094	aquatic macrofossils	0.5206 ± 0.0008	−37.7	3865 ± 15	4320 ± 90	4236–4360, 4365–4408
08LOO-1	32	CURL-10104	aquatic macrofossils	0.5265 ± 0.0009	−32.1	4655 ± 15	5390 ± 70	5317–5331, 5375–5460
08LOO-1	46	CURL-10088	aquatic macrofossils	0.5604 ± 0.0010	−34.5	5155 ± 15	5920 ± 70	6677–6784
08LOO-1	61	CURL-10101	aquatic macrofossils	0.6180 ± 0.0009	−29.5	5525 ± 15	6340 ± 50	6287–6322, 6335–6345, 6369–6393
Goose Lake								
08GOO-3	65	CURL-10437	aquatic macrofossils	0.7393 ± 0.0019	−31.9	2425 ± 25	2520 ± 170	2352–2500, 2596–2613, 2637–2694
08GOO-4	74	CURL-10098	aquatic macrofossils	0.7565 ± 0.0010	−34.7	2240 ± 15	2250 ± 90	2159–2250, 2299–2334
Raven Lake								
08RAV-2	45–46	CURL-11391	Humic acids	0.906 ± 0.0018	−26.5	795 ± 15	710 ± 20	685–732
Iceboom Lake								
08-ICE-5	23	CURL-10083	aquatic macrofossils	0.9591 ± 0.0015	−23.5	335 ± 15	390 ± 80	315–343, 346–413, 418–465
08-ICE-5	36	CURL-10439	aquatic macrofossils	0.7952 ± 0.0019	−27.8	1840 ± 20	1770 ± 60	1713–1825
08-ICE-5	57	CURL-10434	aquatic macrofossils	0.6098 ± 0.0015	−30.7	3980 ± 20	4470 ± 50	4416–4448, 4468–4517
08-ICE-5	70	CURL-10441	aquatic macrofossils	0.4534 ± 0.0013	−30.5	6360 ± 25	7300 ± 120	7184–7188, 7249–7332, 7354–7375, 7386–7414
08-ICE-3	45	CURL-10081	aquatic macrofossils	0.9370 ± 0.0013	−22.4	525 ± 15	530 ± 20	517–548
08-ICE-3	95	CURL-10093	aquatic macrofossils	0.5119 ± 0.0009	−28.4	5380 ± 15	6200 ± 80	6125–6143, 6180–6219, 6234–6275
South Oval Lake								
08SOV-1	6	CURL-10084	aquatic macrofossils	0.9612 ± 0.0013	−25.4	320 ± 15	380 ± 70	308–334, 349–438, 444–455
08SOV-4	63	CURL-10090	aquatic macrofossils	0.4570 ± 0.0008	−27.4	6290 ± 15	7210 ± 40	7171–7258
Merganser Lake								
09MGR-6	163-165	CURL-11369	terrestrial macrofossils	0.8848 ± 0.0016	−28.0	985 ± 15	870 ± 70	802–810, 829–858, 904–934
Alangorliup Lake								
09ALN-2	70–71	CURL-11384	Humic acids	0.5358 ± 0.0011	−26.1	5015 ± 20	5770 ± 110	5661–5757, 5823–5885
Alangorliup Lake Basin								
09GRO-2	NA	CURL-11141	Marine bivalve (Hiatella *arctica*)	0.4162 ± 0.0008	−0.09	7040 ± 20	7410 ± 60	7353–7473

depth on the western side of the lake and is 49 cm long. Core 08SOV-4 (69°18′33″ N, 50°10′5″ W) was collected from 8.90 m depth in the eastern basin and is 86 cm long. Both cores have a relatively thin massive, minerogenic-rich unit that lies immediately beneath ~2 to ~4 cm of organic-rich sediments at the top of the core (Fig. 5). The minerogenic-rich sediments give way to faintly-laminated organic-rich sediments at 6 cm depth in 08SOV-1 and 12 cm depth in 08SOV-4. Core 08SOV-1 contains organic-rich sediments between 6 cm and the its base, at 49 cm, whereas core 08SOV-4 penetrates a lower minerogenic-rich sediment unit at 64 cm depth, which spans to the base of the core at 86 cm. Macrofossils from 6 cm depth in 08SOV-1 yield an age of 320 ± 15 ^{14}C yr BP (380 ± 70 cal yr BP; Table 1). Macrofossils sampled from 63 cm in 08SOV-4 yield a radiocarbon age of 6290 ± 15 ^{14}C yr BP (7210 ± 40 cal yr BP).

4.2. Iceboom Lake

Iceboom Lake (informal name, ~180 m asl) sits ~2 km north of Jakobshavn Isfjord, and ~4 km from the present ice margin (Fig. 6). The lake has a complex outline, several islands, a single outflow to the west, and several minor inflows; Iceboom Lake lies in a 5.18 km^2 catchment. Aerial photographs from 1944, 1953, 1964 and 1985 reveal that Iceboom Lake was glacier fed at least until 1964. An

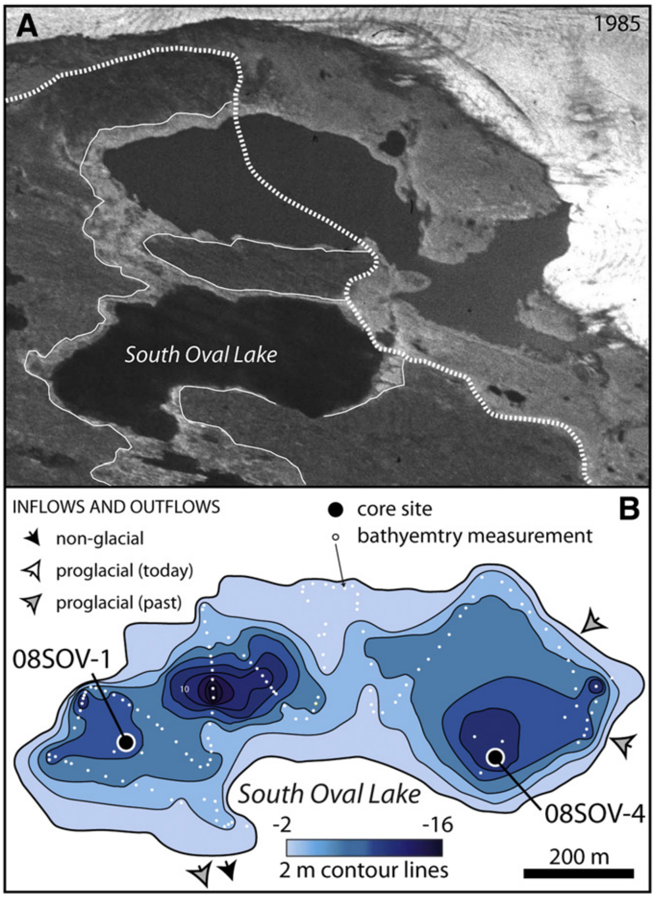

Fig. 4. A. Vertical Air photograph (1985); white lines delimits extent of proglacial lakes when they were fed by ice sheet meltwater during emplacement of historical moraine (white dotted line). B. Bathymetric map of South Oval Lake showing coring locations, inflows and outflows.

abandoned ~200 m-long channel spans between the eastern shoreline and the historical moraine, and a boulder-rich proglacial delta was deposited in the northeastern corner of the lake during the emplacement of the historical moraine ~280 m north of the delta. Iceboom Lake is complex bathymetry, with two relatively large sub-basins ~30–40 m deep and several minor sub-basins. A prominent shoreline ~1 m higher than present lake level reveals much higher inflow during Neoglaciation than today.

We collected five cores from three different locations from Iceboom Lake, and selected two of these for detailed analysis. Core 08ICE-3 (69°13′58″ N, 50°35′00″ W) was collected from 12.21 m depth from a small sub-basin in the southern part of the lake and is 99 cm long. Core 08ICE-5 (69°14′8″ N, 50°1′7″ W) was collected from 3.12 m depth from a shallow sub-basin near the outlet and is 76 cm long. We collected two cores from each of these sites, and chose the longest core from each site for analysis. The fifth core was collected from the eastern basin and is 72 cm long, but appeared through the polycarbonate core tube that it consisted entirely of minerogenic-rich sediments, so it was not analyzed further. The two cores 08ICE-3 and 08ICE-5 show a similar stratigraphy (Fig. 5). Both cores contain a laminated minerogenic-rich unit that lies beneath ~1 cm of organic-rich surface sediment. The base of the minerogenic-rich unit is at 45 cm in 08ICE-3 and 22 cm in 08ICE-5. Beneath this unit lies weakly laminated, organic-rich sediments with sporadic macrofossils. We did not penetrate minerogenic sediments beneath the organic-rich sediments in 08ICE-3, but obtained ~6 cm of minerogenic-rich sediments at the base of 08ICE-5. Macrofossils from core 08ICE-3 from 45 cm and near the core base at 95 cm are 525 ± 15 and 5380 ± 15 ^{14}C yr BP (530 ± 20 and 6200 ± 80 cal yr BP), respectively (Table 1). Macrofossils were dated from core 08ICE-5 at 23 cm depth (335 ± 15 ^{14}C yr BP; 390 ± 80 cal yr BP), 36 cm depth (1840 ± 20 ^{14}C yr BP; 1770 ± 60 cal yr BP), 57 cm depth (3980 ± 20 ^{14}C yr BP; 4470 ± 50 cal yr BP), and 70 cm depth (6360 ± 25 ^{14}C yr BP; 7300 ± 120 cal yr BP; Table 1).

4.3. *Merganser Lake*

Merganser Lake (informal name, 76 m asl) is our closest lake to Jakobshavn Isfjord (Fig. 1); the lake is currently ~19 km from the Jakobshavn Isbræ terminus, and only ~700 m from the historical moraine. The lake has a single inflow that drains a chain of lakes upvalley, and an outflow that drains into Jakobshavn Isfjord; the lake has a long and relatively narrow 9.8 km^2 catchment (Fig. 7). The earliest air photo available, from 1944, reveals an ice-free catchment, but a large, relatively unvegetated proglacial delta that prograded into the lake from the east provides geomorphic evidence that Merganser lake was fed by Jakobshavn Isbræ during the emplacement of the historic moraine. Furthermore, two large channels filled with boulders connect this delta to the moraine, and a deep bedrock gorge and adjacent flooded bedrock surfaces along the lake's outflow channel suggest much higher discharge while the lake was glacier fed. Merganser Lake is up to ~35 m deep and has a relatively simple single-basin bathymetry.

We collected seven cores of varying lengths from Merganser Lake. In order to avoid the likelihood of thick Neoglacial deposits in the lake depocenter, we collected core 09MGR-6 (69° 06′ 51.5′ N, 50° 04′ 40.5″ W) from 15.85 m water depth in a relatively flat-bottomed portion of the lake on the southwestern side distal to the proglacial delta, and chose it for further analysis. The core is 255 cm long, and contains 3 cm of organic-rich sediments on top of 160 cm of coarse minerogenic-rich sediments (up to cobble-sized clasts) to a depth of 163 cm (Fig. 8). Below this depth are organic-rich sediments that become increasingly and gradually minerogenic to the base of the core at 255 cm. Macrofossils are absent from throughout the organic-rich unit, however near the transition from organic-rich to minerogenic-rich sediments at 163 cm depth, and at several higher intervals in the lower section of the minerogenic sediments, are discrete layers of woody macrofossils interpreted to be from terrestrial tundra plants. A single radiocarbon age from macrofossils from the layer at 163 cm is 985 ± 15 ^{14}C yr BP (870 ± 70 cal yr BP; Table 1).

4.4. *Raven Lake*

Proglacial Raven Lake (informal name, ~260 m asl) is one of three lakes in a chain of lakes that begins with Loon and Goose lakes (Fig. 9). Raven Lake has a single 45 m-deep basin and a minor, non-glacial inflow at its southwestern end; this would have been much more significant when Goose Lake was a proglacial lake (see below). The major inflow and single outflow of Raven Lake lie in close proximity in a complex area along the lake's eastern shoreline (Figs. 3 and 9). Raven Lake sits just ~150 m from the historical moraine, but ~3 km from the present ice margin; the lake has an exposed catchment area of 4.7 km^2.

We collected a single core (08RAV-2; 69°4′15″ N, 49°53′1″ W) from 18.37 m depth in the northern part of the lake that is 102 cm long (Fig. 5). Laminated silty-clay comprises the upper 46 cm. Organic-rich sediments span 46–86 cm, and laminated silty-clay is present from 86 cm to the base of the core at 102 cm. The organic-rich sediment unit lacks macrofossils, and we obtained a single

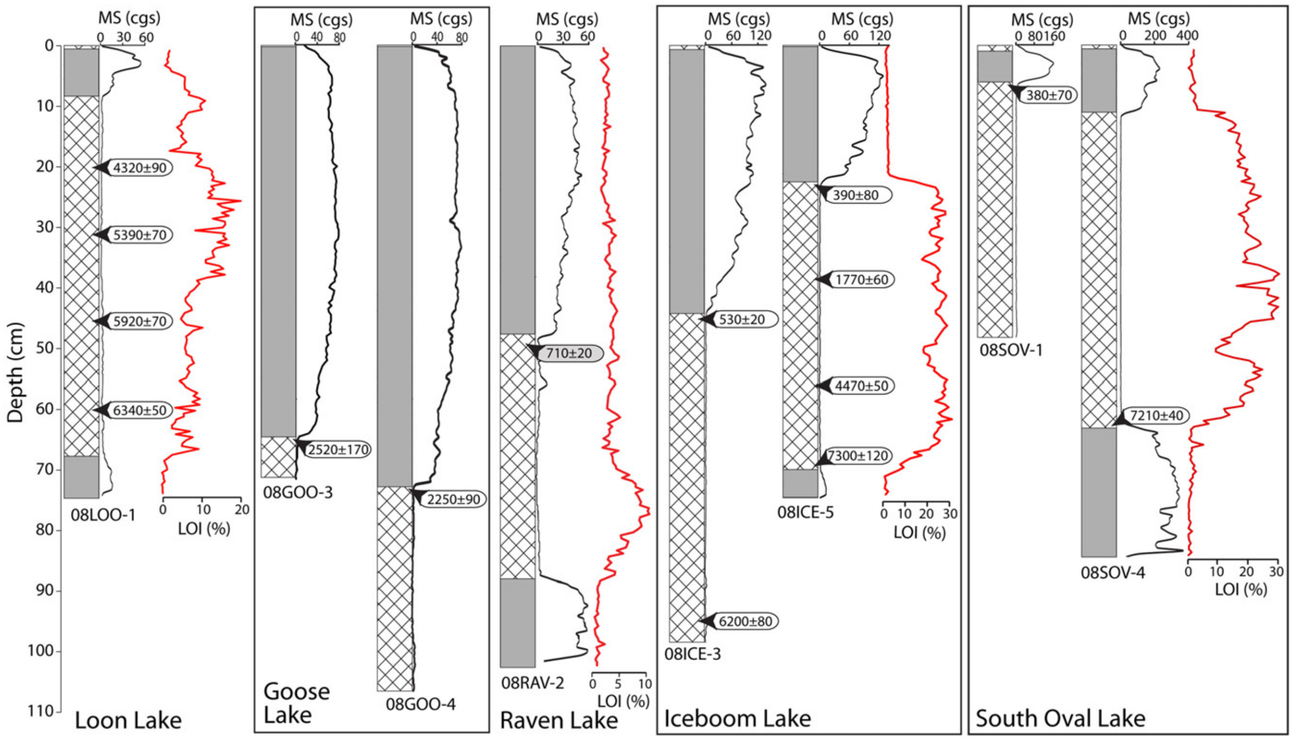

Fig. 5. Lake sediment logs, radiocarbon ages (in cal yr BP), magnetic susceptibility (MS) and loss-on-ignition (LOI). Gray and hachured patterns indicate minerogenic-rich and organic-rich sediments, respectively. Ages with white and gray backgrounds indicate macrofossil- and humic-acid-based radiocarbon ages, respectively. (For interpretation of the references to colour in this figure legend, the reader is referred to the web version of this article).

radiocarbon age on humic acids extracted from bulk sediments at 45–46 cm of 795 ± 15 ^{14}C yr BP (710 ± 20 cal yr BP; Table 1).

4.5. Goose Lake

Goose Lake (informal name, ~275 m asl) has a single outflow that drains into Raven Lake, and a 2.4 km^2 catchment (Fig. 9). The lake lies ~0.6 km from the historical moraine, and ~3.2 km from the present ice sheet margin. Bathymetric data from Goose Lake reveal a 16 m-deep basin and a shallow portion of the lake ~4 m deep at its southwestern side; a rise ~2 m deep separates the main basin and the shallow side of the lake. A minor inflow stream enters Goose Lake along its southwestern shore, and a second inflow stream lies along the eastern shoreline. The eastern inflow crosses an inactive, unvegetated proglacial delta that propagated into the lake during Neoglaciation (Fig. 3). Although Goose Lake does not receive ice sheet meltwater today, aerial photographs from 1959 reveal that Goose Lake was a proglacial lake at least until 1959; the next available aerial photograph imagery of this area from 1985 reveals an ice-free lake basin and clear lake water (Fig. 9). Thus, during maximum Neoglaciation, Goose Lake received a significant inflow from its east.

We collected two adjacent cores from 2.8 m water depth on the bathymetric rise in the southwestern portion of Goose Lake. Core 08GOO-3 (69°03′39″ N, 49°54′14″ W) is 75 cm long; 08GOO-4 is 110 cm long (Fig. 5). Organic-rich sediments are present at the top 0.5 cm of both cores. Laminated silty-clay extends to 65 cm in 08GOO-3 and to 74 cm in 08GOO-4. The base of the each core is composed of weakly laminated organic-rich sediments with aquatic macrofossils. Macrofossils from within 1 cm of the lower organic-sediment/minerogenic-sediment contact were dated from each core, yielding radiocarbon ages of 2425 ± 25 and 2240 ± 15 ^{14}C yr BP (2520 ± 170 and 2250 ± 90 cal yr BP; Table 1).

4.6. Loon Lake

Loon Lake (informal name, 277 m asl; Fig. 9) is the highest of three adjacent lakes, lying above Goose and Raven lakes. Loon Lake is completely free of ice sheet meltwater today, but geomorphic evidence reveals a meltwater channel that originates from the historic moraine and enters Loon Lake near its outflow. Loon Lake lies ~0.4 km from the historical moraine and ~3 km from the present ice margin and has a 1.6 km^2 catchment. The lake has multiple sub-basins; bathymetry was measured in a small portion of the lake near its outflow at its northeastern edge; a maximum depth of 16 m was recorded.

We collected a single, 75 cm-long core from 15.8 m depth in Loon Lake (08LOO-1; 69° 3′29.35″ N, 49°54′57.80″ W; Fig. 9). Organic-rich sediments are present in the top 1.5 cm of the core (Fig. 5). This overlays a layer of massive minerogenic-rich sediment, followed by a sharp contact at 7 cm, below which is organic-rich sediments that continues to 68 cm. The basal 7 cm consists of laminated minerogenic-rich sediment. Four ^{14}C ages obtained from macrofossils are from 20 cm (3865 ± 15 ^{14}C yr BP; 4320 ± 90 cal yr BP), 32 cm (4655 ± 15 ^{14}C yr BP; 5390 ± 70 cal yr BP), 46 cm (5155 ± 15 ^{14}C yr BP: 5920 ± 70 cal yr BP) and 61 cm (5525 ± 15 ^{14}C yr BP; 6340 ± 50 cal yr BP; Table 1).

4.7. Eqaluit taserssuat

Eqaluit taserssuat (~11 m asl) is the southernmost lake that we cored (Fig. 10). The proglacial lake lies north of Alangorliup Sermia, a large tidewater outlet glacier that feeds the southern tributary fjord of Jakobshavn Isfjord, but is fed by the land-based ice margin ~5 km to its east (Fig. 1). This is the largest lake that we cored, and lies in the largest catchment with an exposed area of ~72 km^2 and an unknown area that projects inland beneath the GIS. Two

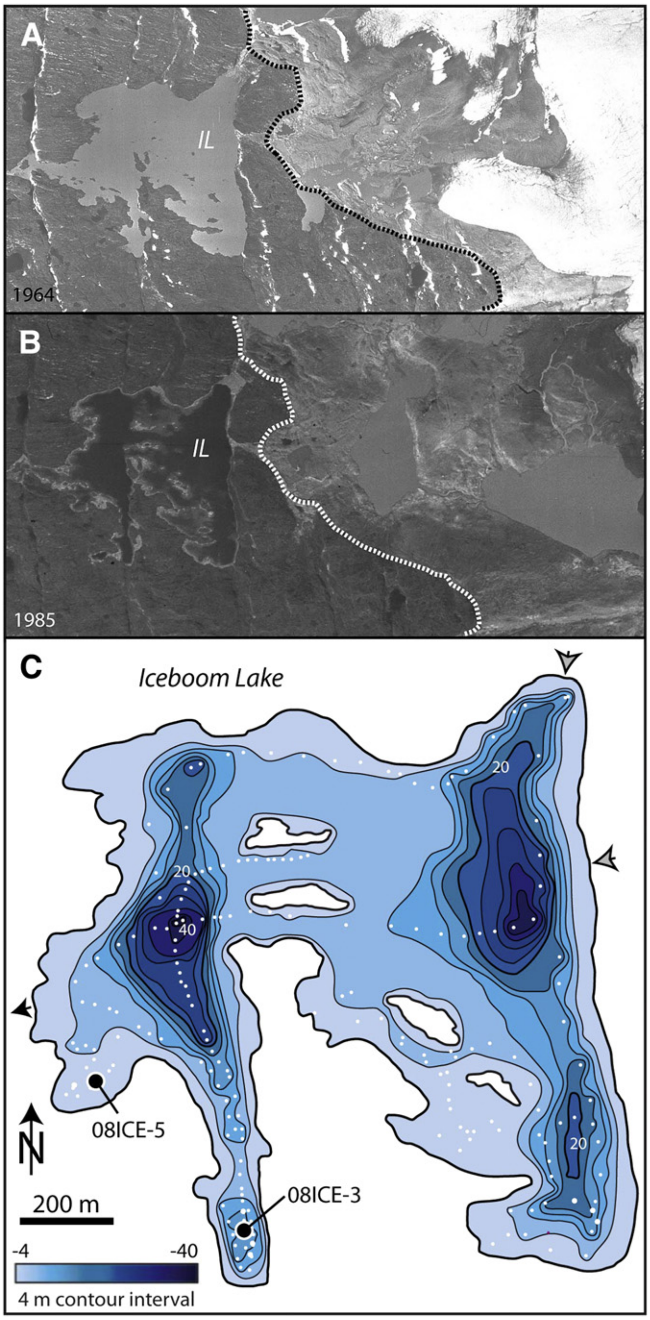

Fig. 6. Vertical Air photographs showing Iceboom Lake (IL) as a proglacial lake in 1964 (A) and non-glacial lake by 1985 (B); dotted lines indicate location of the historic moraine. C. Bathymetric map of Iceboom Lake shows coring locations.

significant proglacial stream systems enter the lake's southeastern shoreline in the same area, and the lake is drained by a single channel at its western side. Geomorphic evidence reveals a marine limit around the lake at ~20 m asl, indicating that Eqaluit taserssuat is an emerged marine basin. A radiocarbon age from a single, articulated Hiatella *arctica* bivalve from raised marine deposits near the lake shoreline (68° 58′ 27.9″ N, 50° 04′ 24.1″ W; 12 m asl) is 7040 ± 20 ^{14}C yr BP (7410 ± 60 cal yr BP; Table 1). Due to windy conditions, we were only able to investigate the southern embayment of Eqaluit taserssuat, from which we measured bathymetry and collected multiple sediment cores. This portion of the lake bottom is relatively flat and broad, and up to ~32m deep. No sill was found between the sub-basin and the main lake body, which was measured with one transect to be ~24 m deep and relatively flat.

We collected one surface core and two long sediment cores, one of which was chosen for further investigation. 09ALN-2 (68°59′5.6″ N, 50°7′54.4″ W) was collected from 18.54 m depth and is 305 cm long (Fig. 8). The upper 68 cm of the core is comprised of minerogenic-rich sediments with relatively high MS values. A relatively thin section of organic-rich sediments exists from 69 to 75 cm depth; this unit has the lowest MS values of the core and has relatively high LOI values. Beneath the organic-rich sediment unit is a minerogenic-rich sediment unit that spans the rest of the core to its base. The organic-rich sediments are devoid of macrofossils; a single radiocarbon age obtained from humic acids extracted from bulk sediments at 70–71 cm depth is 5015 ± 20 ^{14}C yr BP (5770 ± 110 cal yr BP; Table 1).

5. Discussion

5.1. Interpreting lake sediment sequences

The sediment stratigraphy from all lakes that we investigated near Jakobshavn Isbræ is generally similar, and displays alternating lithologies of organic-rich sediments with high LOI and low MS values, and minerogenic-rich sediments with low LOI and high MS values. The sharp transitions between these alternating sediment units exhibit behavior typical of proglacial-threshold lakes. This characteristic, combined with the glacial-geomorphic context of each lake basin, and the transition of some of these lakes from proglacial to non-glacial captured in historical imagery, point to the minerogenic-rich units being glacially-derived. The cores that penetrated minerogenic basal sediments record regional deglaciation during the early Holocene. All cores contain a single unit of organic-rich sediments spanning various durations of the middle Holocene, which indicate ice-free conditions between deglaciation and Neoglaciation, and all cores contain a single unit of minerogenic-rich sediments that represent the advance of the GIS following its minimum middle Holocene extent. All sites but two (Raven Lake and Eqaluit taserssuat) became non-glacial lakes again during the 20th century, and have thin units of organic-rich sediments at their surface.

Basal radiocarbon ages from four sediment cores from three different lakes constrain the timing of regional deglaciation. Two radiocarbon ages are from the contact between basal minerogenic-rich sediments and overlying organic-rich sediments; these are 7300 ± 120 and 7210 ± 40 cal yr BP from Iceboom Lake (08ICE-5) and South Oval Lake (08SOV-4), respectively. In addition, the dated bivalve from raised marine deposits near the shoreline of Eqaluit taserssuat constrains deglaciation of that region to at or before 7410 ± 60 cal yr BP. Together, the radiocarbon ages suggest that this ~50 km-long sector of the ice margin deglaciated roughly synchronously ~7.4 to ~7.2 ka to a position at or inland of the 20th century ice margin configuration.

Organic-rich sediments deposited during the middle Holocene record deposition under non-glacial conditions at all sites. Even the large proglacial Eqaluit taserssuat apparently became a non-glacial lake during the middle Holocene, indicated by the thin unit of organic-rich sediments and sharp transition back to minerogenic-rich sediments. We interpret the lower minerogenic-rich unit in Eqaluit taserssuat as proglacial marine sediments, and correlate it with the raised marine sediments rimming the lake basin that date to 7410 ± 60 cal yr BP. The MS values of this unit steadily decrease toward the contact with the overlying organic-rich sediment unit, suggesting an increasing distance between the marine embayment and the ice source. The deposition of proglacial marine sediments was followed by emergence of the basin and its transition to a non-

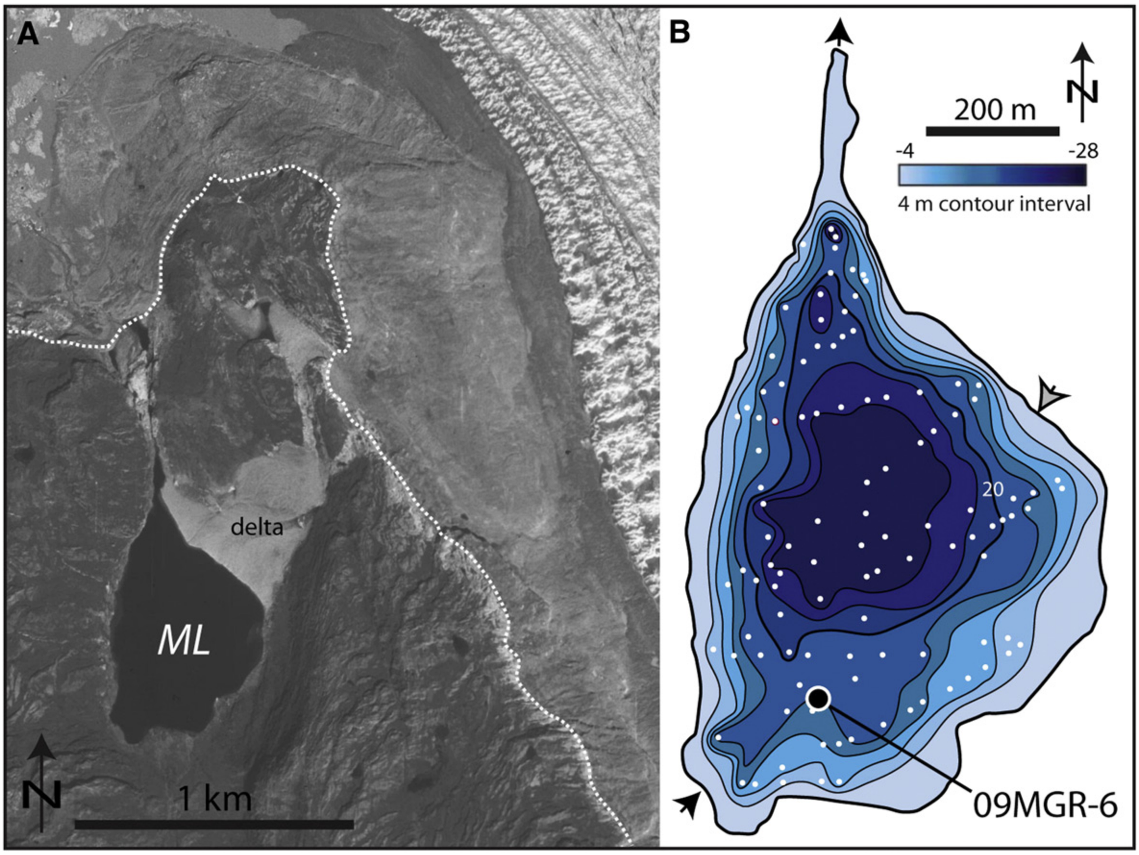

Fig. 7. Vertical Air photograph (1959) and accompanying bathymetric map of Merganser Lake (ML) showing coring locations. White dotted line delimits the historic moraine.

glacier-fed lake, indicated by the abrupt increase in LOI values. Relative sea level curves from the region (Long et al., 2006) reveal rapid emergence upon deglaciation (>10 m/1000 years), and suggest that it took less than 1000 years for Eqaluit taserssuat to emerge out of the sea. Although this core is poorly dated, the single radiocarbon age of 5770 ± 100 cal yr BP from the organic-rich sediment unit, combined with the thinness of the unit and knowledge about emergence rates during that time period, suggest that Eqaluit taserssuat was only a non-glacial lake for a short period of time during the middle Holocene. In addition, the radiocarbon age is from bulk sediments, which have been shown to be too old elsewhere where bulk sediments and macrofossils have been dated at the same levels (Wolfe et al., 2004). In west Greenland lakes, Kaplan et al. (2002) found the offset to be 230 years, McGowan et al. (2003) found the offset to be 405 years, and Bennike et al. (2010) found the offset to be 100–200 years; all intervals were from the middle Holocene. Thus, we can only estimate the non-glacial interval in Eqaluit taserssuat to span a relatively short period of time around ~6000–5000 cal yr BP. The other lakes that we studied have much smaller catchment areas (<10 km^2), and contain much thicker organic-rich sediment units. None of the organic-rich sediment units are interrupted by minerogenic-rich sediment layers, and multiple radiocarbon ages from throughout the organic-rich sediments at multiple lake sites (Loon and Iceboom lakes) suggest continuous organic sedimentation until Neoglaciation.

All lakes record Neoglacial expansion of the GIS by the deposition of ice sheet meltwater-derived minerogenic-rich sediments above organic-rich sediments. For Eqaluit taserssuat, the single lake that we cored with a large catchment, this occurred during the middle Holocene following a brief interval when its catchment was ice-free. The remainder of the lakes, all with relatively small catchment sizes, suggests that the timing of when this sector of the GIS reached its near-present configuration is variable within the study area. South of Jakobshavn Isbræ, the contact is dated at Goose Lake, which indicates that the ice margin advanced into Goose Lake's catchment shortly after 2250 ± 90 cal yr BP (the younger of the two radiocarbon ages from just below the contact at Goose Lake). Based on the location of the GIS when Goose Lake transitioned back to a non-glacial lake between 1959 and 1985, we estimate that the GIS came within ~3 km of Goose Lake ~2250 cal yr BP. The uppermost radiocarbon age from Loon Lake (4320 ± 90 cal yr BP) is consistent with the possibility that this portion of the GIS reached its near-present ice margin by ~2250 ± 90 cal yr BP. Neighboring Raven Lake apparently did not transition into a proglacial lake until after 710 ± 20 cal yr BP. This age is based on bulk sediments (see above), thus, it is possible that the GIS advanced into the lake catchment several hundred years after 710 ± 20 cal yr BP.

It seems surprising that the neighboring Raven and Goose lakes became proglacial lakes at such different times. However, the present inflow/outflow area of Raven Lake is complex (Fig. 3), and it is possible that Raven Lake did not transition into a proglacial lake until sediments filled a basin that then made glaciofluvial deposition into Raven Lake possible. Thus, Raven Lake's eastern catchment boundary was at its outflow upon ice advance, but the drainage basin became reorganized during glaciation, and it currently extends to the present ice margin. Alternatively, the Ravel Lake catchment did not change, but rather the radiocarbon ages from Goose Lake are complicated by a hiatus between uppermost organic-rich sediments and the minerogenic unit, which could be due to erosion upon initial deposition of Neoglacial sediments in the lake basin. This seems unlikely, however, given the coring

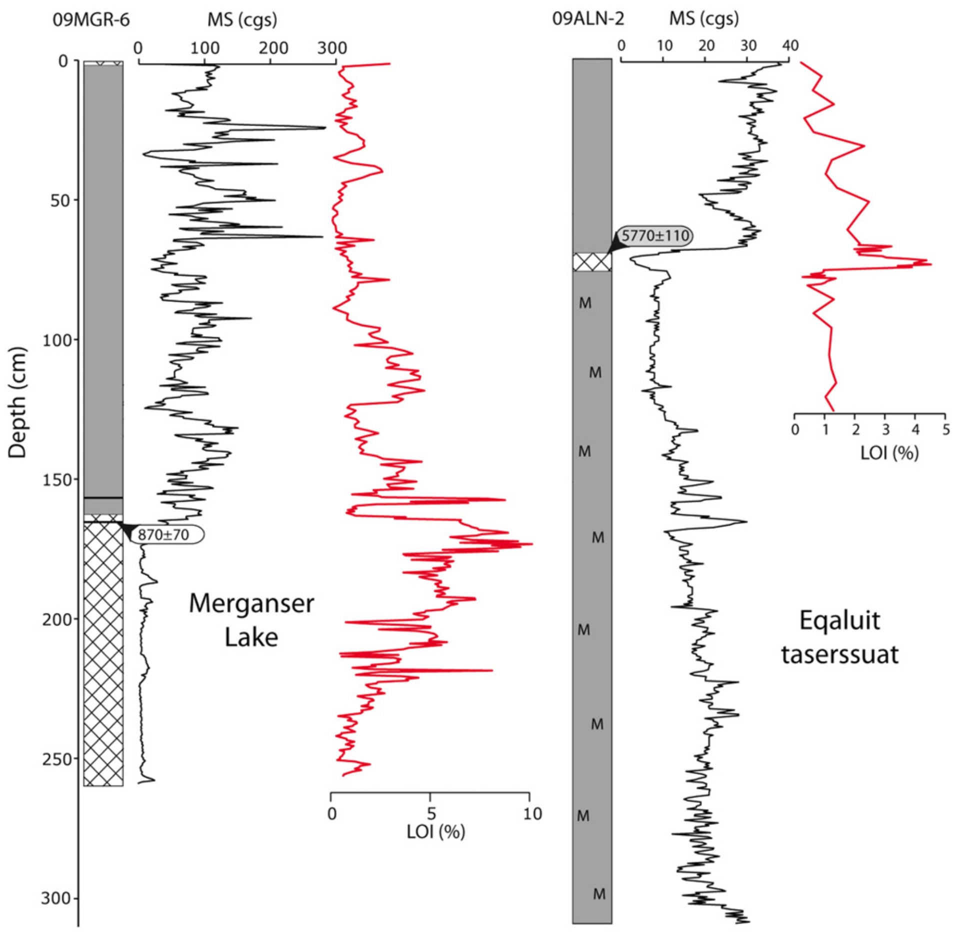

Fig. 8. Lake sediment logs, radiocarbon dates (in cal yr BP), magnetic susceptibility (MS) and loss-on-ignition (LOI). Gray and hachured patterns indicate minerogenic-rich and organic-rich sediments, respectively. Thin black lines indicate layers of terrestrial macrofossils; M indicates minerogenic-rich marine sediment. Ages with white and gray backgrounds indicate macrofossil- and humic-acid-based radiocarbon ages, respectively. (For interpretation of the references to colour in this figure legend, the reader is referred to the web version of this article).

location on a rise in the lake bottom on the distal portion of the lake basin from the inflow delta.

Closer to Jakobshavn Isbræ are Merganser and Iceboom lakes, south and north of Jakobshavn Isfjord, respectively. The single radiocarbon age for the contact between organic-rich and minerogenic-rich sediments from Merganser Lake of 870 ± 70 cal yr BP is from a layer of terrestrial macrofossils that we interpret to have been deposited in the lake during an inwash event. This age for the arrival of Jakobshavn Isbræ is significantly older than at Iceboom Lake, where radiocarbon ages from immediately below the Neoglacial sediments are 390 ± 80 and 530 ± 20 cal yr BP. Based on when Iceboom Lake became non-glacial in the 20th century (between 1964 and 1985), we suggest that the ice margin was within 3 km of Iceboom Lake just after ~400 cal yr BP, which is the younger of the two uppermost radiocarbon ages in Iceboom Lake sediment cores. We interpret the age from Merganser Lake as being too old and that the terrestrial macrofossils spent some time accumulating in the catchment before being suddenly washed into the lake, which is implied by the mode of deposition (Thomas et al., 2010). Thus, we treat the radiocarbon age from Merganser Lake as a maximum age constraint for the arrival of Jakobshavn Isbræ. Taken together, we constrain the timing of advance of Jakobshavn Isbræ to be within the LIA, probably ~400 cal yr BP. Finally, the radiocarbon age from the South Oval Lake of 380 ± 70 cal yr BP indicates the time when this small catchment was breached by the land-based ice margin in that region. Because the historical moraine rests on South Oval Lake's eastern drainage divide, we suggest that this sector of the ice sheet essentially reached its maximum extent sometime soon after ~400 cal yr BP.

5.2. Jakobshavn Isbræ and surrounding ice margins through the Holocene

Taken together, our results suggest that the GIS retreated behind the position of its Neoglaciation-maximum ice margin ~7.4–7.2 ka. This age agrees with several independent age assessments for the retreat of this sector of the GIS. Long et al. (2006) provide basal radiocarbon ages from lakes at mid-Isfjord suggesting that deglaciation there took place prior to ~7700 yr ago. The oldest radiocarbon-dated reworked marine fauna remains from historical moraines in the region are 6120 ± 140 cal yr BP (Weidick et al., 1990; Weidick and Bennike, 2007), indicating that deglaciation had taken place by then. The most direct dating of ice sheet retreat, however, comes from the ^{10}Be ages reported in Young et al. (in press) from glacially-eroded bedrock surfaces just beyond the historical moraine, which cluster at 7.4 ± 0.1 ka.

Between deglaciation and Neoglaciation, this portion of the GIS retreated an unknown distance inland. Our evidence from Eqaluit taserssuat indicates that the GIS margin there had deglaciated far enough inland to be completely out of its catchment. The challenge is knowing how far inland the catchment penetrates; given the overall size and widening geometry of the catchment toward the

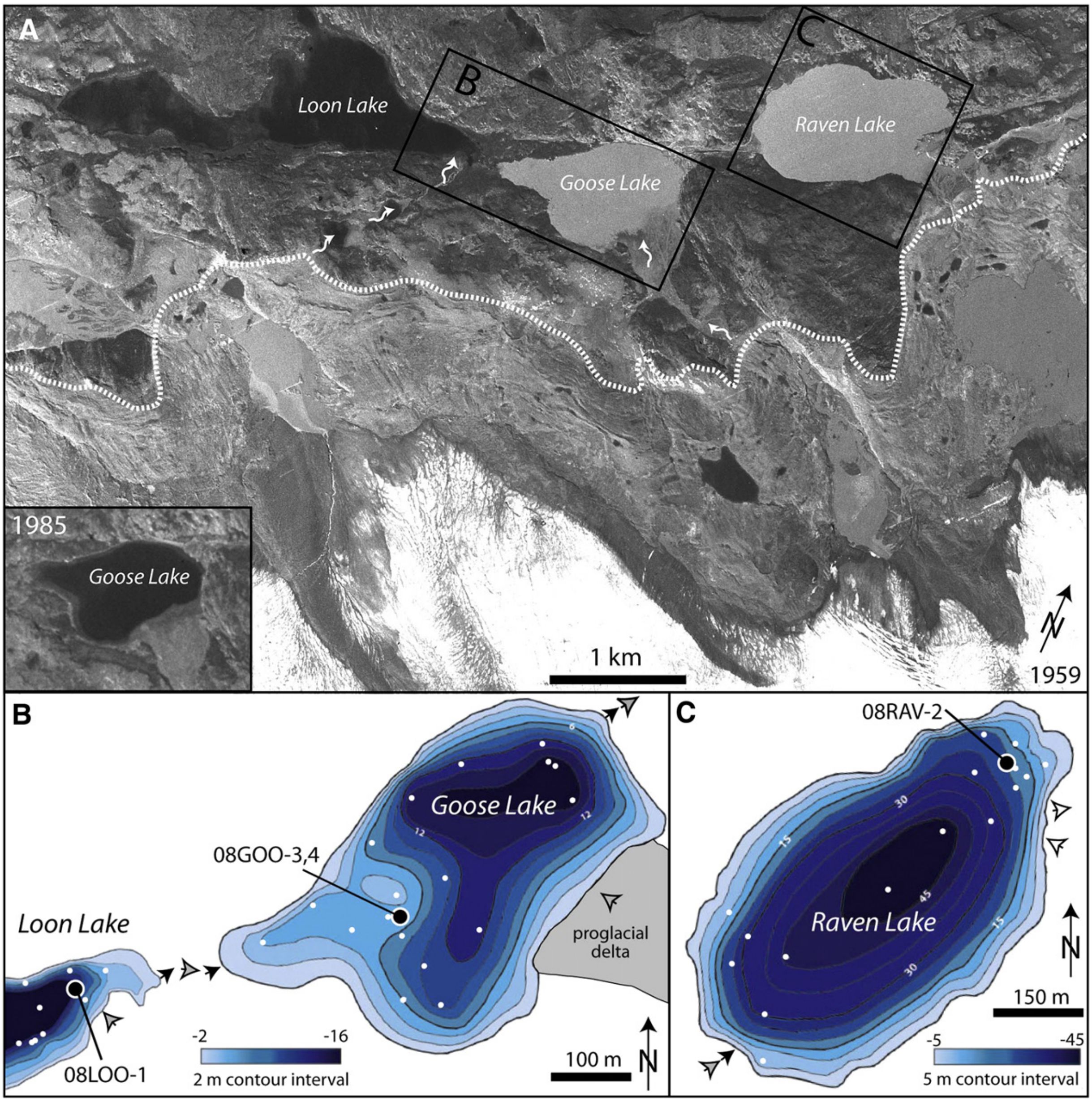

Fig. 9. A. Vertical air photograph of Loon, Goose and Raven lakes acquired in 1964. White dotted line demarcates location of historical moraine; white arrows indicate proglacial meltwater routes. Inset shows Goose Lake in 1985 air photograph. B. and C. show lake bathymetry with coring locations.

current ice margin, it could perhaps extend 10 km or more eastward beneath the ice margin. Regardless of how far inland the catchment extends, the lake sediments from Eqaluit taserssuat suggest peak minimum ice conditions during the middle Holocene, perhaps ~6–5 ka. Based on the presence of marine fauna remains in the historical moraine and general knowledge about sub-ice geometry, Weidick et al. (1990) suggested that this sector of the GIS was ~15 km inland of the ice margin location in the 1980s. Numerical ice sheet models based on geophysical inversions of relative sea level data, climate records, and glacial geologic data depict a significant reduction in ice extent along the southwestern sector of the GIS from ~61° N to ~70 °N (Letreguilly et al., 1991; Van Tatenhove et al., 1995; Tarasov and Peltier, 2002, 2003; Fleming and Lambeck, 2004; Simpson et al., 2009). The general timing and magnitude of inland retreat differ among the models, and only broadly capture the ice sheet changes from our reconstruction. Some models reconstruct little to no inland retreat in the Jakobshavn region (e.g., Simpson et al., 2009), whereas others depict significant retreat (~100 km; Tarasov and Peltier, 2002) but during a time period (e.g., 8000 yr ago) incompatible with our reconstruction.

The radiocarbon ages of marine fauna reworked into the historical moraines in the Jakobshavn region span from 6120 ± 140 cal yr BP to 2340 ± 310 cal yr BP (Weidick and Bennike, 2007). The young end of the range of radiocarbon ages can be interpreted as a maximum age constraint for the when Jakobshavn Isbræ and its neighboring marine outlet glaciers neared their Neoglacial maxima. The youngest age of ~2300 cal yr BP is consistent with the radiocarbon ages from Goose Lake, and together suggest that at least one portion of the GIS margin may have been near its Neoglaciation-maximum limit as early as ~2300 cal yr BP. The middle Holocene reduction and late Holocene

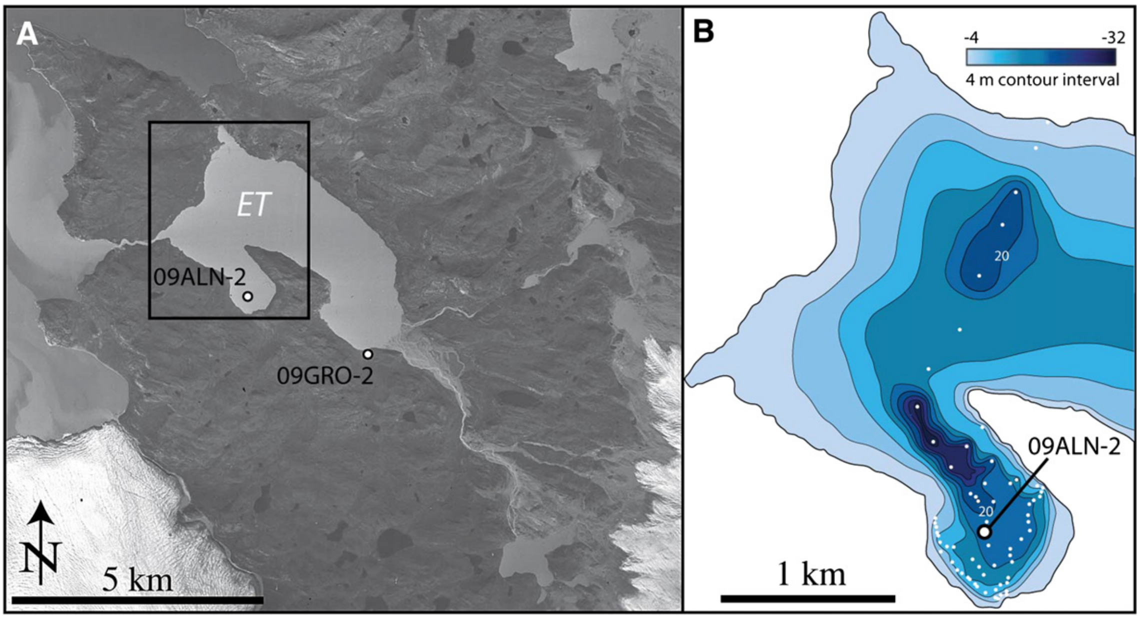

Fig. 10. A. Vertical air photograph (1985) of Eqaluit taserssuat (ET) showing coring location of 09ALN-2 and location of raised marine deposits (09GRO-2). B. Bathymetric map of Eqaluit taserssuat showing core site.

expansion of ice volume is also recorded by relative sea level data from the Disko Bugt region. Long et al. (2006) summarize the relative sea level record from the region, which reveals landscape submergence initiating ~3000 cal yr BP. This submergence is interpreted to record the expansion of the western GIS during Neoglaciation.

The culmination of Neoglaciation of this sector of the GIS occurred during the LIA. After extensive surveying of the historical moraine near all of our study lakes, we found very little vegetation cover, and sparse colonization of the lichen *Rhizocarpon geographicum* with small maximum diameters (<14 mm). Thus, despite evidence that the ice margin near Goose Lake may have been near its Neoglacial maximum as early as ~2300 cal yr BP, there is no evidence for moraines that pre-date the LIA (Weidick and Bennike, 2007). Ice-rafted debris and foraminifera faunal records from marine sediment cores near the mouth of Jakobshavn Isfjord suggest that Jakobshavn Isbræ had a similar extent between ~2200 and ~1700 cal yr BP as today (Lloyd, 2006). We have evidence of the earlier episode of glacial conditions captured in Goose Lake. On the other hand, the record from Lloyd (2006) begins ~2200 cal yr BP, thus it is unknown when the relatively cool conditions near the Jakobshavn Isfjord mouth initiated. Lloyd (2006) also has evidence for a relatively extensive Jakobshavn Isbræ after ~500 cal yr BP, which is consistent with the bulk of our evidence for the timing of when maximum Neoglacial conditions were achieved.

5.3. Neoglaciation in southwestern Greenland

To place the ice sheet reconstructions of the Jakobshavn ice margin into a broader context, we briefly review evidence for the timing of Neoglaciation elsewhere around southwestern Greenland. Neoglaciation occurred along the entire west Greenland coast (Kelly, 1980; Weidick, 1993; Kelly and Lowell, 2009). Numerous records depict Late Holocene cooling initiating from ~5 to ~3 ka (Funder and Weidick, 1991; Levac et al., 2001; Kaplan et al., 2002; Lloyd et al., 2007). However, in most areas the maximum Neoglacial extent appears to have been achieved during the LIA (Weidick, 1968; Kelly, 1980; Kaplan et al., 2002). Some sectors of the GIS may have attained a maximum extent prior to the LIA. Moraines of the Narssarssuaq stade, southernmost Greenland, apparently formed shortly before 2 ka (Bennike and Sparrenbom, 2007), and Forman et al. (2007) suggest that a moraine beyond the LIA moraine along the Kangerlussuaq sector of the GIS may have been deposited ~2000 yr ago. Several studies have used radiocarbon ages of marine material reworked into LIA moraines to constrain time periods of smaller-than-present ice extents reveals a broad range of ages from scattered locations around Greenland between ~9 and ~2 ka (Kelly, 1980; Weidick et al., 2004; Weidick and Bennike, 2007; Bennike, 2008). The lower age range of these radiocarbon ages provides maximum ages for the Neoglacial advance of the GIS. Finally, the relative sea level from throughout southwest Greenland suggests an increasing ice load initiating between ~3 and ~1 ka (Kelly, 1980; Long et al., 2006, 2009; Mikkelsen et al., 2008; Woodroffe and Long, 2009).

Thus, although most ice sheet sectors contain maximum Neoglacial moraines that date to the LIA, there is some evidence that the western GIS was near or at its LIA extent as early as ~2000 yr ago. It appears from the evidence at Goose Lake that the ice margin south of Jakobshavn Isbræ advanced to within ~3 km of its Neoglacial maximum position ~2250 cal yr BP. Furthermore, it appears that the GIS did not retreat out of Goose Lake's catchment anytime between ~2250 and the 20th century, including during the Medieval Warm Period. If correct, the ongoing retreat of the ice margin south of Jakobshavn Isbræ may be unprecedented within the last >2000 years.

5.4. Implications for Jakobshavn Isbræ dynamics

The lacustrine-based records of Jakobshavn Isbræ's fluctuations over the Holocene generated here extend our knowledge of Jakobshavn Isbræ change back in time, and suggest that its behavior on centennial and longer timescales generally matches the behavior of the broader western GIS through the Holocene. Similar to the observational record revealing that Greenland's major ice streams behave more erratically than their adjacent margins, we find that there may indeed be some spatial complexity in ice margin change in the paleo-record. The magnitude that the

Jakobshavn Isbræ terminus advanced during the LIA was greater than the adjacent land-based ice margins. Furthermore, although the ice margin south of Jakobshavn Isbræ began expanding as early as the middle Holocene and approached its Neoglaciation-maximum extent ~2300 cal yr BP, evidence from our study lakes north of Jakobshavn Isbræ suggest that this sector of the GIS did not near its Neoglaciation-maximum until within the LIA. On the other hand, given our low sample density of only seven lakes, and only one lake in a large catchment, it is alternatively possible that the ice margin north of Jakobshavn Isbræ was near its current position earlier during Neoglaciation. In any case, despite a significant dynamical component of Jakobshavn Isbræ's behavior witnessed on sub-decadal timescales, and its significantly larger response to the LIA cold perturbation relative to its adjacent ice margins, the paleo-record reveals that Jakobshavn Isbræ sensitively responds to climate change (Young et al., in press).

6. Conclusion

Radiocarbon-dated sediment sequences from multiple proglacial-threshold lakes near Jakobshavn Isbræ constrain the timing of early Holocene deglaciation, the duration that this sector of the western GIS was smaller than its present configuration, and the timing of its advance during Neoglaciation. These continuous lacustrine records corroborate, but provide closer age control than, the non-continuous record of radiocarbon-dated reworked bivalves from historical moraines in the region. Our radiocarbon chronology suggests deglaciation ~7300 cal yr BP and we reconstruct a smaller-than-present ice configuration until ~2300 cal yr BP for the ice margin south of Jakobshavn Isbræ, and until ~400 cal yr BP for the ice margin north of Jakobshavn Isbræ. The evidence from Eqaluit taserssuat, the single large catchment proglacial lake that we cored, suggests that even it became non-glacial, implying significant inland retreat culminating ~6–5 ka. Our reconstruction of Neoglaciation is consistent with relative sea level data from the region that reveal late Holocene ice expansion, and with marine sediment studies near the mouth of Jakobshavn Isfjord that suggest extensive ice phases ~2000 cal yr BP and after ~500 cal yr BP.

Reconstructions of ice margin change from proglacial-threshold lakes is one of very few approaches with the potential to constrain smaller-than-present ice sheet extent. Our study lakes have relatively small catchments and thus, only record the time when ice approaches its maximum configuration. Lakes residing within larger drainage basins that tap more deeply behind the present GIS margin, like Eqaluit taserssuat, have the potential to constrain ice margin advance and retreat across larger distances. As subglacial bedrock mapping improves, information about the size of sub-ice drainage basins and threshold locations will become available, which will ultimately improve reconstructions from proglacial-threshold lakes. In any case, because the response of the GIS to Holocene climate change, including during the interval of warmer-than-present temperatures, is relevant for understanding the response of the GIS to future climate change, there is some urgency to develop more records like these. This study benefits from a substantial amount of prior research in the Jakobshavn Isbræ region, however, this approach can be applied in other locations around Greenland that lack this framework of prior research.

Acknowledgments

We thank Devin Bedard and Stefan Truex for help in the laboratory, and Chad Wolak and Scott Lehman at the INSTAAR radiocarbon lab. We are grateful for outstanding field support during the field campaigns provided by CH2MHill Polar Field Services; funding provided by NSF Geography and Spatial Sciences (NSF-BCS-0752848). Finally, we thank Tom Lowell and an anonymous reviewer for helping to strengthen this manuscript.

References

ACIA, 2005. Arctic Climate Impact Assessment: ACIA Scientific Report. Cambridge University Press, Cambridge, UK/New York, NY, USA, 1042 pp.
Alley, R.B., Clark, P.U., Huybrechts, P., Joughin, I., 2005. Ice-sheet and sea-level changes. Science 310, 456–460.
Alley, R.B., Andrews, J.T., Brigham-Grette, J., Clarke, G.K.C., Cuffey, K.M., Fitzpatrick, J.J., Funder, S., Marshall, S.J., Miller, G.H., Mitrovica, J.X., Muhs, D.R., Otto-Bliesner, B.L., Polyak, L., White, J.W.C., 2010. History of the Greenland ice sheet: paleoclimatic insights. Quaternary Science Reviews 29, 1728–1756.
Bennike, O., 2008. An early Holocene Greenland whale from Melville Bugt, Greenland. Quaternary Research 69, 72–76.
Bennike, O., Bjorck, S., 2002. Chronology of the last recession of the Greenland ice sheet. Journal of Quaternary Science 17, 211–219.
Bennike, O., Sparrenbom, C.J., 2007. Dating of the Narssarssuaq stade in southern Greenland. Holocene 17, 279–282.
Bennike, O., Hansen, K.B., Knudsen, K.L., Penny, D.N., Rasmussen, K.L., 1994. Quaternary marine stratigraphy and geochronology in central west Greenland. Boreas 23, 194–215.
Bennike, O., Anderson, N.J., McGowan, S., 2010. Holocene palaeoecology of south-west Greenland inferred from macrofossils in sediments of an oligosaline lake. Journal of Paleoliminology 43, 787–798.
Box, J.E., Bromwich, D.H., Veenhuis, B.A., Bai, L.S., Stroeve, J.C., Rogers, J.C., Steffen, K., Haran, T., Wang, S.H., 2006. Greenland ice sheet surface mass balance variability (1988–2004) from calibrated polar MM5 output. Journal of Climate 19, 2783–2800.
CAPE Last Interglacial Project Members, 2006. Last Interglacial Arctic warmth confirms polar amplification of climate change. Quaternary Science Reviews 25, 1383–1400.
Chapin, F.S., Sturm, M., Serreze, M.C., McFadden, J.P., Key, J.R., Lloyd, A.H., McGuire, A.D., Rupp, T.S., Lynch, A.H., Schimel, J.P., Beringer, J., Chapman, W.L., Epstein, H.E., Euskirchen, E.S., Hinzman, L.D., Jia, G., Ping, C.L., Tape, K.D., Thompson, C.D.C., Walker, D.A., Welker, J.M., 2005. Role of land-surface changes in Arctic summer warming. Science 310, 657–660.
Csatho, B., Schenk, T., van der Veen, C.J., Krabill, W., 2007. Intermittent thinning of Jakobshavn Isbræ, west Greenland, since the Little ice age. Journal of Glaciology 54, 131–144.
Daigle, T.A., Kaufman, D.S., 2009. Holocene climate inferred from glacier extent, lake sediment and tree rings at Goat Lake, Kenai Mountains, Alaska, USA. Journal of Quaternary Science 24, 33–45.
Forman, S.L., Marin, L., Van der Veen, C., Tremper, C., Csatho, B., 2007. Little ice age and neoglacial landforms at the inland ice margin, Isunguata Sermia, Kangerlussuaq, west Greenland. Boreas 36, 341–351.
Fleming, K., Lambeck, K., 2004. Constraints on the Greenland Ice Sheet since the Last Glacial Maximum from sea-level observations and glacial-rebound models. Quaternary Science Reviews 23, 1053–1077.
Funder, S., Weidick, A., 1991. Holocene boreal molluscs in Greenland – palaeoceanographic implications. Palaeogeography, Palaeoclimatology, Palaeoecology 85, 123–135.
Funder, S., Hansen, L., 1996. The Greenland ice sheet: a model for its culmination and decay during and after the last glacial maximum. Bulletin of the Geological Society of Denmark 42, 137–152.
Funder, S., Jennings, A., Kelly, M., 2004. Middle and late Quaternary glacial limits in Greenland. In: Elhers, J., Gibbard, P.L. (Eds.), Quaternary Glaciations – Extent and Chronology, Part II, pp. 4250–4430.
Holland, D.M., Thomas, R.H., Young, B.D., Ribergaard, M.H., Lyberth, B., 2008. Acceleration of Jakobshavn Isbræ triggered by warm subsurface ocean waters. Nature Geoscience 1, 659–664.
Howat, I.M., Joughin, I., Scambos, T.A., 2007. Rapid changes in ice discharge from Greenland outlet glaciers. Science 315, 1559–1561.
IPCC, 2007. Climate change 2007: the physical science basis. In: Solomon, S., Qin, D., Manning, M., Chen, Z., Marquis, M., Averyt, K.B., Tignor, M., Miller, H.L. (Eds.), Contribution of Working Group I to the Fourth Assessment Report of the Intergovernmental Panel on Climate Change. Cambridge University Press, Cambridge, UK/New York, NY, USA, 996 pp.
Joughin, I., Abdalati, W., Fahnestock, M., 2004. Large fluctuations in speed on Greenland's Jakobshavn Isbræ glacier. Nature 432, 608–610.
Kaplan, M.R., Wolfe, A.P., Miller, G.H., 2002. Holocene environmental variability in southern Greenland inferred from lake sediments. Quaternary Research 58, 149–159.
Kaufman, D.S., Ager, T.A., Anderson, N.J., Anderson, P.M., Andrews, J.T., Bartlein, P.J., Brubaker, L.B., Coats, L.L., Cwynar, L.C., Duvall, M.L., Dyke, A.S., Edwards, M.E., Eisner, W.R., Gajewski, K., Geirsdottir, A., Hu, F.S., Jennings, A.E., Kaplan, M.R., Kerwin, M.N., Lozhkin, A.V., MacDonald, G.M., Miller, G.H., Mock, C.J., Oswald, W.W., Otto-Bliesner, B.L., Porinchu, D.F., Ruhland, K., Smol, J.P., Steig, E.J., Wolfe, B.B., 2004. Holocene thermal maximum in the western Arctic (0–180 degrees W). Quaternary Science Reviews 23, 529–560.
Kaufman, D.S., Schneider, D.P., McKay, N.P., Ammann, C.M., Bradley, R.S., Briffa, K.R., Miller, G.H., Otto-Bliesner, B.L., Overpeck, J.T., Vinther, B.M., Arctic Lakes 2k Project Members, 2009. Recent warming reverses long-term arctic cooling. Science 325, 1236–1239.

Kelly, M., 1980. The status of the Neoglacial in western Greenland. Rapprt Grønlands Geologiske Undersøgelse 96, 24.
Kelly, M.A., Lowell, T.V., 2009. Fluctuations of local glaciers in Greenland during latest Pleistocene and Holocene time. Quaternary Science Reviews 28, 2088–2106.
Krabill, W., Hanna, E., Huybrechts, P., Abdalati, W., Cappelen, J., Csatho, B., Frederick, E., Manizade, S., Martin, C., Sonntag, J., Swift, R., Thomas, R., Yungel, J., 2004. Greenland ice sheet: increased coastal thinning. Geophysical Research Letters 31.
Letreguilly, A., Reeh, N., Huybrechts, P., 1991. The Greenland Ice Sheet through the last glacial–interglacial cycle. Palaeogeography, Palaeoclimatology, Palaeoecology 90, 385–394.
Levac, E., de Vernal, A., Blake Jr., W., 2001. Sea-surface conditions in northernmost Baffin Bay during the Holocene. Palynological evidence. Journal of Quaternary Science 16, 353–363.
Lloyd, J.M., 2006. Late Holocene environmental change in Disko Bugt, west Greenland: interaction between climate, ocean circulation and Jakobshavn Isbræ. Boreas 35, 35–49.
Lloyd, J.M., Park, L.A., Kuijpers, A., Moros, M., 2005. Early Holocene paleoceanography and deglacial chronology of Disko Bugt, west Greenland. Quaternary Science Reviews 24, 1741–1755.
Lloyd, J.M., Kuijpers, A., Long, A., Moros, M., Park, L.A., 2007. Foraminiferal reconstruction of mid- to late-Holocene ocean circulation and climate variability in Disko Bugt, West Greenland. The Holocene 17, 1079–1091.
Long, A.J., 2009. Back to the future: Greenland's contribution to sea-level change. GSA Today 19, 4–10.
Long, A.J., Roberts, D.H., 2002. A revised chronology for the 'Fjord stade' moraine in Disko Bugt, west Greenland. Journal of Quaternary Science 17, 561–579.
Long, A.J., Roberts, D.H., 2003. Late Weichselian deglacial history of Disko Bugt, west Greenland, and the dynamics of the Jakobshavns Isbræ ice stream. Boreas 32, 208–226.
Long, A.J., Roberts, D.H., Dawson, S., 2006. Early Holocene history of the west Greenland ice sheet and the GH-8.2 event. Quaternary Science Reviews 25, 904–922.
Long, A.J., Woodroffe, S.A., Dawson, S., Roberts, D.H., Bryant, C.L., 2009. Late Holocene relative sea level rise and the Neoglacial history of the Greenland Ice Sheet. Journal of Quaternary Science 24, 345–359.
McGowan, S., Ryves, D.B., Anderson, N.J., 2003. Holocene records of effective precipitation in West Greenland. The Holocene 13, 239–249.
McNeely, R., Dyke, A.S., Southon, J.R., 2006. Canadian Marine Reservoir Ages, Preliminary Data Assessment. Open File 5049. Geological Survey Canada, pp. 3.
Meier, M.F., Dyurgerov, M.B., Rick, U.K., O'Neel, S., Pfeffer, W.T., Anderson, R.S., Anderson, S.P., Glazovsky, A.F., 2007. Glaciers dominate eustatic sea-level rise in the 21st century. Science 317, 1064–1067.
Mikkelsen, N., Kuijpers, A., Arneborg, J., 2008. The Norse in Greenland and late Holocene sea-level change. Polar Record 44, 45–50.
Miller, G.H., Alley, R.B., Brigham-Grette, J., Fitzpatrick, J.J., Polyak, L., Serreze, M.C., White, J.W.C., 2010. Arctic amplification: can the past constrain the future? Quaternary Science Reviews 29, 1779–1790.
Nesje, A., 1992. A piston corer for lacustrine and marine sediments. Arctic and Alpine Research 24, 257–259.
Nick, F.M., Vieli, A., Howat, I.M., Joughin, I., 2009. Large-scale changes in Greenland outlet glacier dynamics triggered at the terminus. Nature Geoscience 2, 110–114.
Otto-Bliesner, B.L., Marshall, S.J., Overpeck, J.T., Miller, G.H., Hu, A., CAPE Last Interglial Project Members, 2006. Simulating polar amplification of orbital forcing for the last interglacial. Science 311, 1751–1753.
Overpeck, J.T., Otto-Bliesner, B.L., Miller, G.H., Muhs, D.R., Alley, R., Kiehl, J.T., 2006. Paleoclimatic evidence for future ice sheet instability and rapid sea level rise. Science 311, 1747–1750.
Parizek, B.R., Alley, R.B., 2004. Implications of increased Greenland surface melt under global-warming scenarios: ice sheet simulations. Quaternary Science Reviews 23, 1013–1027.
Pfeffer, W.T., Harper, J.T., O'Neel, S., 2008. Kinematic constraints on glacier contributions to 21st century sea-level rise. Science 321, 1340–1343.
Pritchard, H.D., Arthern, R.J., Vaughn, D.G., Edwards, L.A., 2009. Extensive dynamic thinning on the margins of the Greenland and Antarctic ice sheets. Nature 461, 971–975.
Rignot, E., Kanagaratnam, P., 2006. Changes in the velocity structure of the Greenland ice sheet. Science 311, 986–990.
Rignot, E., Box, J.E., Burgess, E., Hanna, E., 2008. Mass balance of the Greenland ice sheet from 1958 to 2007. Geophysical Research Letters 35, L20502. doi:10.1029/2008GL035417.
Simpson, M.J.R., Milne, G.A., Huybrechts, P., Long, A.J., 2009. Calibrating a glaciological model of the Greenland Ice Sheet from the Last Glacial Maximum to present-day using field observations of relative sea level and ice extent. Quaternary Science Reviews 28, 1631–1657.
Stuiver, M., Reimer, P.J., Reimer, R.W., 2005. CALIB 6.0 [WWW program and documentation].
Tarasov, L., Peltier, W.R., 2002. Greenland glacial history and local geodynamic consequences. Geophysical Journal International 150, 198–229.
Tarasov, L., Peltier, W.R., 2003. Greenland glacial history, borehole constraints, and Eemian extent. Journal of Geophysical Research 108, 2143. doi:10.1029/2001JB001731.
Thomas, E.K., Szymanksi, J.S., Briner, J.P., 2010. The evolution of Holocene alpine glaciation inferred from lacustrine sediments on northeastern Baffin Island, Arctic Canada. Journal of Quaternary Science 25, 146–161.
Thomas, R., Frederick, E., Krabill, W., Manizade, S., Martin, C., 2006. Progressive increase in ice loss from Greenland. Geophysical Research Letters 33.
Van Tatenhove, F.G.M., Van der Meer, J.J.M., Huybrechts, P., 1995. Glacial-geological geomorphological research in West Greenland used to test an ice-sheet. Quaternary Research 44, 317–327.
Weidick, A., 1968. Observations on some Holocene glacier fluctuations in west Greenland. Meddelelsser Om Grønland 165, 202.
Weidick, A., 1974. C14 dating of survey material performed in 1974. Rapport Grønlands Geologiske Undersøgelse 75, 19–20.
Weidick, A., 1992. Jakobshavn Isbræ area during the climatic optimum. Rapport Grønlands Geologiske Undersøgelse 155, 67–72.
Weidick, A., 1993. Neoglacial change of ice cover and the related response of the Earth's crust in west Greenland. Rapport Grønlands Geologiske Undersøgelse 159, 121–126.
Weidick, A., 1994. Historical fluctuations of calving glaciers in south and west Greenland. Rapport Grønlands Geologiske Undersøgelse 161, 73–79.
Weidick, A., Bennike, O., 2007. Quaternary glaciation history and glaciology of Jakobshavn Isbræ and the Disko Bugt region, west Greenland: a review. Geological Survey of Denmark and Greenland Bulletin 14, 78.
Weidick, A., Oerter, H., Reeh, N., Thomsen, H.H., Thorning, L., 1990. The recession of the inland ice margin during the Holocene climatic optimum in the Jakobshavn-Isfjord area of west Greenland. Global and Planetary Change 82, 389–399.
Weidick, A., Kelly, M., Bennike, O., 2004. Late Quaternary development of the southern sector of the Greenland Ice Sheet, with particular reference to the Qassimiut lobe. Boreas 33, 284–299.
Wolfe, A.P., Miller, G.H., Olsen, C.A., Forman, S.L., Doran, P.T., Holmgren, S.U., 2004. Geochronology of high Latitude Lake sediments. In: Pienitz, R., Douglas, M., Smol, J. (Eds.), Long-term Environmental Change in Arctic and Antarctic Lakes. Springer, Dordrecht, The Netherlands.
Woodroffe, S., Long, A.J., 2009. Salt marshes as archives of recent relative sea level change in west Greenland. Quaternary Science Reviews 28, 1750–1761.
Young, N.E., Briner, J.P., Stewart, H.A.M., Axford, Y., Csatho, B., Rood, D.H., Finkel, R.C., The response of Jakobshavn Isbræ to Holocene climate change. Geology, in press.
Zwally, H.J., Giovinetto, M.B., Li, J., Cornejo, H.G., Beckley, M.A., Brenner, A.C., Saba, J.L., Yi, D.H., 2005. Mass changes of the Greenland and Antarctic ice sheets and shelves and contributions to sea-level rise: 1992–2002. Journal of Glaciology 51, 509–527.